processes

Article

Study on Flow and Heat Transfer in Single Rock Fractures for Geothermal Heat Extraction

Duanru Li [1,2], Gang Liu [1,*] and Shengming Liao [1,*]

1 School of Energy Science and Engineering, Central South University, Changsha 410083, China
2 School of Civil Engineering, Hunan University of Technology, Zhuzhou 412007, China
* Correspondence: gangliu@csu.edu.cn (G.L.); smliao@csu.edu.cn (S.L.)

Abstract: A full understanding of the fluid flow and heat transfer behaviors within a single fracture is important for geothermal heat extraction. In this study, models of single fractures with varying aperture and inner surface roughness (characterized by fractal dimension) are constructed, and a compound fracture aperture (CFA) is proposed to describe the coupled effect of fracture aperture and inner surface roughness. The effect of the fluid flow Reynolds number on heat transfer was investigated as it ranged from 4.84 to 145.63. The results show that the overall heat transfer coefficient (OHTC) in a single fracture significantly increases with the rise in fluid velocity and the compound fracture aperture. Particularly, the OHTC in a single fracture with an inner surface fractal dimension of 2.09 can be up to 1.215 times that of a parallel flat fracture when the flow velocity reaches 0.18 m/s. Moreover, for a fracture with a smaller CFA, enhancing the fracture aperture plays a decisive role in increasing the OHTC. Aperture emerges as a more sensitive optimization parameter for efficient heat extraction compared to the flow velocity. Meanwhile, based on simulation results, a convective heat transfer correlation equation is derived to provide more accurate estimates of the OHTC in rock fractures with different geometries and morphological features.

Keywords: geothermal energy; enhanced geothermal system; overall heat transfer coefficient; roughness fracture; single fracture

check for updates

Citation: Li, D.; Liu, G.; Liao, S. Study on Flow and Heat Transfer in Single Rock Fractures for Geothermal Heat Extraction. *Processes* **2024**, *12*, 363. https://doi.org/10.3390/pr12020363

Academic Editor: Jiaqiang E

Received: 11 January 2024
Revised: 7 February 2024
Accepted: 7 February 2024
Published: 9 February 2024

1. Introduction

Geothermal energy, being both clean and renewable, has attracted increasing attention worldwide for its development and utilization. To achieve heat extraction from the hot dry rock (HDR) of deep geothermal resources, the Enhanced Geothermal System (EGS) has been proposed [1]. This involves constructing artificial geothermal reservoirs in low-permeability HDR through engineering techniques such as hydraulic fracturing [2], as shown in Figure 1. This process aims to establish pathways for fluid flow and heat exchange within deep geothermal reservoirs, enabling the extraction of high-quality heat for direct utilization in urban heating or power generation. Thus, the overall heat production of an EGS strongly relies on the efficient connection of the fracture systems [3]. A single fracture serves as the basic component of the fracture network and is critical for simulation, analysis and evaluation [4]. Therefore, it is necessary to sufficiently understand the fluid flow and heat transfer characteristics through a single fracture during the heat extraction process from deep geothermal reservoirs.

The process of fluid flow and heat transfer within a single fracture involves a series of effect factors, including the flow rate, the thermophysical properties of the working fluid and rock and the geometry and morphology of the fracture, as well as the pressure and temperature of the confining environment, etc. [5]. Recently, many studies have been conducted on these affecting factors, with experiments and simulations serving as the main research methods in these studies. The experimental studies are primarily focused on the water-flowing and heat transfer characteristics within a single fracture, and most of the results show that either larger flow rates or rougher fracture surfaces significantly influence the heat transfer efficiency of water flowing through the rock [6–9]. Bai et al. considered the average temperature distribution of the fracture surface as linear [10] or polynomial [11] based on their experimental data. The lab tests data from Huang et al. [12] also suggested the conclusion that the outlet temperature is almost linear with the initial rock temperature and high flow rate increasing the temperature of the fluid, which are obtained when the fluid become stable, within about 10 min. He et al. [13] found that the local heat transfer coefficient (LHTC) distribution mainly depends on the fracture surface roughness, followed by aperture and flow rate. Moreover, Luo et al. [14] found that the energy exchange rate increases continuously with the rock temperature, with an effective stress ratio of 1:2. Li et al. [15] indicated that the effects of the dissolution reaction on fracture surface morphology exists but it is extremely small for heat transfer. The heat transfer characteristics are also affected by the environmental conditions of deep geothermal reservoirs. According to the experimental results of Shu et al. [16], the confining pressure is the primary factor that controls hydraulic properties, while the reservoir temperature is the primary factor that controls heat transfer characteristics. These experimental results have laid a solid foundation for further quantitative research. A cylindrical rock model is the most commonly used in experiments for flow and heat transfer within a single fracture. Although some recent studies revealed that heat transfer properties vary with the geometry of the rock model [5], the lack of monitoring of temperature distribution within the fracture voids still prevents a comprehensive understanding of flow and heat transfer in roughness fractures.

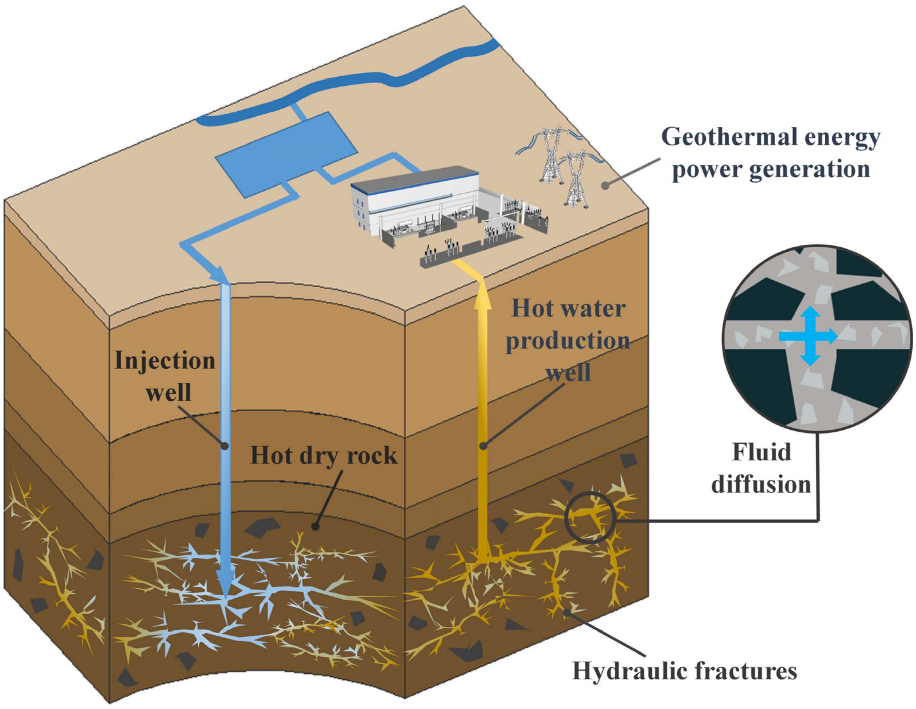

Figure 1. Schematic diagram of geothermal energy utilization with EGS.

Compared to experiments, simulations offer greater convenience and flexibility in modeling complicated geometries and flow conditions, as well as providing a more intuitive representation of the heat transfer process within the fracture. The effects of fracture geometry parameters and surface roughness remain a difficult and focal issue in numerical simulations [17]. The roughness of the fracture walls was commonly described by joint roughness coefficient (JRC) curves [18,19] or geometric parameters with certain mathematical rules [20–22]. However, the study of both the JRC and roughness elements was mainly limited to two-dimensional (2D) models [23]. With the understanding of the anisotropic nature of heat transfer in fractures [24], three-dimensional (3D) models were also constructed in some simulations. He et al. [25] proposed a morphology condition factor to account for the effect of surface roughness on heat transfer intensity. However, fractures with heterogeneous apertures were constructed in their subsequent simulations [26]. Chen et al. [5] developed an empirical model to describe the relationship between the normalized heat transfer coefficient and the hydraulic aperture. Moreover, in integrated studies and analysis, a formula for the calculation of the overall heat transfer coefficient (OHTC) was proposed or improved to evaluate the heat transfer ability between the fluid and rock within an entire fracture [10,27,28]. The approximate value of the OHTC calculated by Shaik et al. is around 900 $W/(m^2 \cdot K)$ [23]. Zhao et al. [29] developed analytical solutions for convective heat transfer on the assumption of a flat plate for a single fracture. He et al. [26] studied the heat transfer coefficient by solving the temperature distribution of a cylindrical rock sample in the form of an integral function. According to the numerical results of Zhang et al. [30], the overall Nusselt number (*Nu*) obtained was larger in roughness fractures with a larger Reynolds number (*Re*), due to the disturbance effect of boundary layer development. Although the impact of fracture geometric dimensions and surface morphology characteristics has been further demonstrated through numerical investigations [25], the effect of the coupling of these two factors on the fluid and heat transfer characteristics remains uncertain.

In summary, to further understand the coupled fluid–solid heat transfer issues within a single fracture, it is necessary to delve into the effects of fracture geometry and inner surface morphology on fluid flow and heat transfer, particularly when these two factors are coupled. In this study, models of single fractures with different fractal dimension (D) are constructed, and a compound fracture aperture (CFA) is proposed to describe the fracture aperture and inner surface roughness. Through a series of simulations for the heat transfer process under various flow conditions, we discuss the fluid flow and heat transfer characteristics within a single fracture. By quantifying the coupling relationship between the heat transfer capacity of the fracture and the influencing factors, we establish a convective heat transfer correlation equation with better generality, which can provide guidance for and optimize the development of deep geothermal energy extraction systems.

2. Numerical Model

2.1. Model Setup

The numerical model was built up as a cylinder with 50 mm diameter and 100 mm height, based on the rock experimental model by Bai et al. [31]. By splitting the cylinder along the length direction, a rock fracture channel with a certain aperture was formed. As shown in Figure 2a, when fluid flows through the fracture, we consider that there is only one inlet and one outlet to the fracture, and that the fluid is in complete contact with the inner wall surface of the fracture. The heat is directly transmitted from the outer wall of the rock to the inner wall surface of the fracture, as shown in Figure 2b, and the fluid–solid-coupled heat transfer is realized by continuously heating the flowing fluid. The heat distribution and water flow processes in the fracture are developed as a transient behavior.

The controllable geometric features of the fracture channel models mainly include the inner wall surface morphology and the channel aperture, etc. The numerical model of a single fracture channel is hypothetically formed by constructing the fracture surface and moving it along the normal direction. Table 1 lists the numerical models and parameters for single fractures established in this study. Figure 3 shows four types of regularly changing fracture inner surface morphologies. Amongst them, s1~s3 are roughness surfaces with regularly changing features established based on the self-affine characteristics of the rock fracture surface morphologies [32]. The morphological features of the roughness fracture surface are comprehensively characterized by fractal dimension (D) and the undulation height of matrix points (Z) [13]; more specific parameters can be found in Table 1. The surface of s0 was built for verification, which is from the experimental sample model of Ma et al. [4], with the joint roughness coefficient (JRC) [6] values of the surface ranging from 16 to 18.

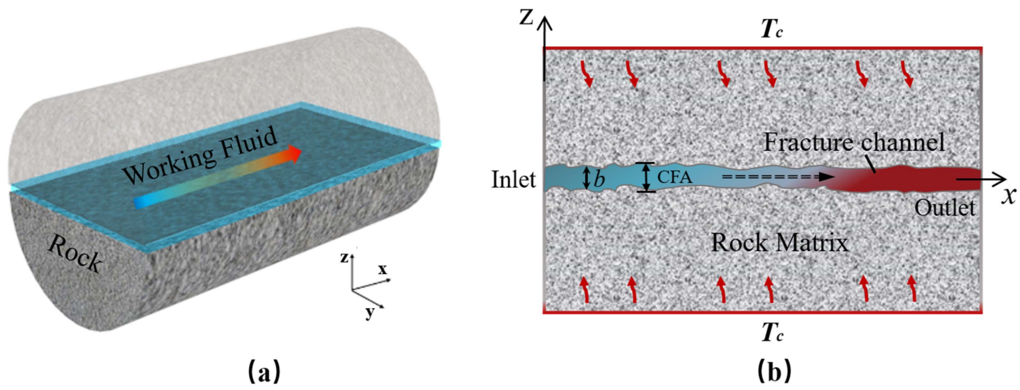

Figure 2. Numerical models of the single rock fracture, (**a**) 3D single fracture model, (**b**) schematic of the rock fracture channel and heat transfer.

Table 1. The parameters of the numerical models for a single fracture.

The Single Fracture Models	Fracture Surfaces	Characterization of the Fracture Surface	Projected Sizes of the Fracture Surface (mm)	Aperture (b/mm)	The CFA with Corresponding Apertures (mm)
F_{Sp}	sp	Parallel plate	50 × 100	0.1, 0.2, 0.3, 0.4, 0.5	0.100, 0.200, 0.300, 0.400, 0.500
F_{S1}	s1	D = 2.003			0.100, 0.201, 0.301, 0.402, 0.502
F_{S2}	s2	D = 2.018			0.100, 0.201, 0.301, 0.402, 0.502
F_{S3}	s3	D = 2.090			0.106, 0.212, 0.317, 0.423, 0.529
F_{S0}	s0	JRC: 16–18		0.2	--

In order to analyze the mechanism of fracture morphology's effect on the heat transfer characteristics of fluid flow through a single fracture, it is necessary to quantify the morphology characteristics of the three-dimensional fracture channel. This study used a compound fracture aperture (CFA) to describe the inner surface roughness and aperture of a single fracture surface. The CFA is expressed as:

$$\mathrm{CFA} = \frac{V_f}{S_n} \tag{1}$$

where V_f is the volume of the single fracture (mm^3) and S_n is the projected area of the upper- or lower-roughness wall surface in a single fracture (mm^2).

2.2. Numerical Governing Equations and Boundary Conditions

The convective heat transfer of the working fluid in the rock fracture is a combination of both the macroscopic behavior of thermal convection (heat transfer between the fluid and solid surface) and the microscopic behavior of heat conduction (heat transfer perpendicular to the direction of fluid flow) [12]. Thereby, it is coupled between the water and rock at the inner wall surface of the fracture. The finite element code, COMSOL™ (version 6.2), was employed in this study for the simulation of the fluid flow and heat transfer process through a single fracture.

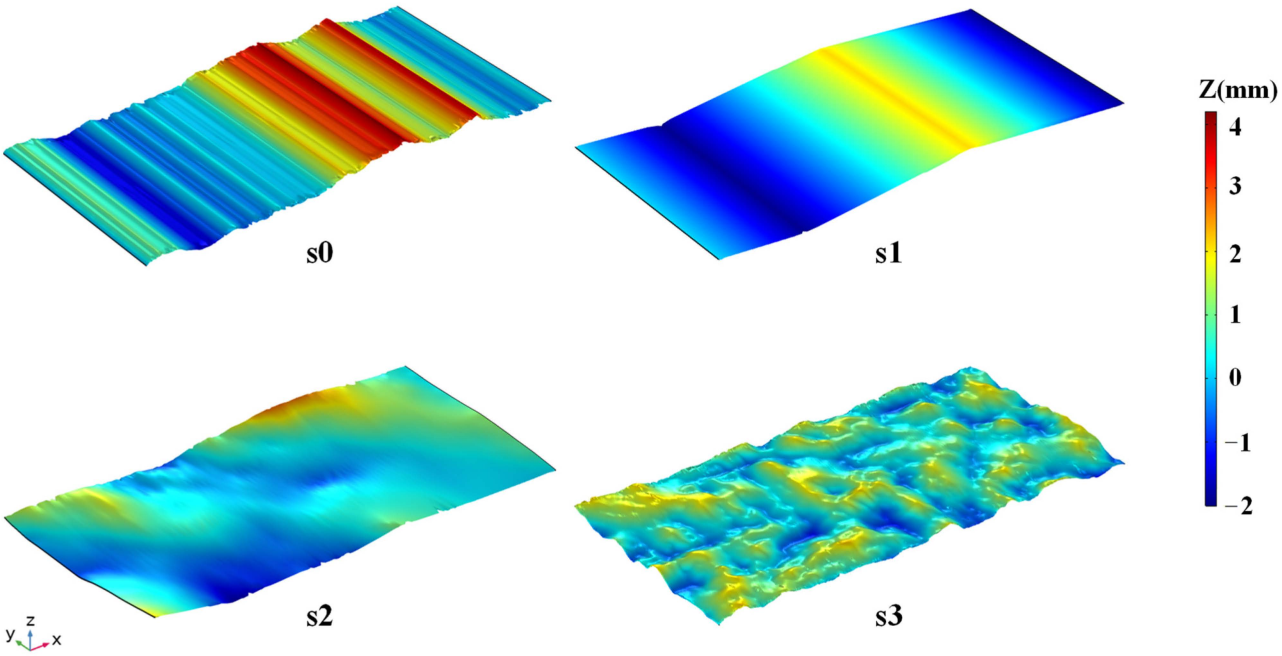

Figure 3. Four inner surface morphologies for single fractures.

When water is the liquid phase with a small variation range of temperature, it is considered that the fluid flow is incompressible and there is no phase change during the flow process. As some lab tests data have shown, the transient temperatures of the fracture walls and the fluid become stable within about 10 min [12], and the simulation results by solving the Navier–Stokes equations agree well with the flow-testing results [33]. Meanwhile, the main flow of the fluid within a rough single fracture was found to be laminar in many experimental results [34,35], and there was no creep flow and no fully developed turbulent flow as the turbulence occurred only near the curved wall [34,36]. At the same time, they found that viscous resistance is more dominant during the fluid flow in the fracture than inertial resistance [37,38]. Moreover, the flow pattern can be further determined by the value of the Reynolds number (*Re*), which is calculated as [30]:

$$Re = \frac{ud_e}{\nu} \quad (2)$$

where u is the fluid flow velocity (m/s), specified as constant values (0.01~0.18 m/s) at the inlet boundary; d_e stands for the characteristic dimension of the single fracture (mm) ($d_e = 4A_c/P_w$, where A_c is the average cross-sectional area of the fracture in the flow direction, m^2, and P_w is the average wetting perimeter, m); and ν is the kinematic viscosity coefficient of the water (m^2/s). After calculation, the values of *Re* ranged from 4.84 to 145.63 for all cases in this study, which is lower than the minimum critical *Re* values proposed by most scholars [38–41].

Therefore, laminar flow was adopted for the flow status in this study. It is reasonable to assume that the single-phase water flow in the fracture is a steady, continuous flow and follows the Navier–Stokes equations. The continuity equation and momentum conservation equation are represented below:

$$\frac{\partial \rho}{\partial t} + \nabla\cdot(\rho u) = 0 \quad (3)$$

$$\rho\frac{\partial u}{\partial t} + \rho(u\cdot\nabla)u = -\Delta P + \nabla\cdot\left[\mu\nabla u + \mu(\nabla u)^T\right] + \rho f \quad (4)$$

where ρ stands for the density of the fluid and varies with temperature; P is the hydraulic pressure; μ is the dynamic viscosity of the fluid; f is the body force tensor; t is the time; and T is the shear stress tensor.

The process of heat transfer inside the rock satisfies the differential equation of thermal conduction. The temperature of the fracture surface and fluid tends to be stable after a certain time. The heat transfer equation for rock in a steady state is expressed as:

$$\rho_r C_{P,r} \frac{\partial T_r}{\partial t} + \nabla \cdot (-k_r \nabla T_r) = 0 \tag{5}$$

where ρ_r is the density of the rock; $C_{P,r}$ is the constant pressure-specific heat capacity of the rock; and T_r, k_r are the temperature and thermal conductivity of the rock.

The governing equation for the heat transfer between the fluid and rock is:

$$\rho_r C_{p,r} \frac{\partial T_r}{\partial t} + \rho_f C_{P,f} u \cdot \nabla T_f + \nabla \cdot \left(-k_f \nabla T_f \right) = 0 \tag{6}$$

where ρ_f is the density of water; $C_{P,f}$ is the constant pressure-specific heat capacity of water; and T_f, k_f are the temperature and thermal conductivity of water.

The model material properties are defined as granite, which has a density of 2620 kg/m^3, a specific heat capacity of 757 J/(kg·K) and a heat conductivity of 2.784 W/(m·K) [19]. Due to the extremely low porosity of the granite, the rock matrix is assumed to be impermeable, ensuring that there was no-flow and no-slip on its two inner wall surfaces. The outer wall was maintained as a constant temperature of 373.15 K, with the fluid–solid-coupled heat transfer interface taken into account for the inner surfaces, while the other wall surfaces were adiabatic. The water flow was considered to have no filtration loss through the wall of the fracture. Given that fluid properties, including density, dynamic viscosity, specific heat capacity, and thermal conductivity coefficient, vary with temperature, especially within the wide range of temperatures found in deep reservoirs, these properties of water were considered temperature-dependent (Figure 4). For each simulation case, the temperature of the fluid at the fracture inlet was set to 313.15 K, and the transient average outlet temperatures for the water were recorded as T_{out}. The outlet boundary of the water was free outflow, while the environment pressure of the fracture was subject to a fixed boundary of 30 MPa. The nominal velocities for working fluid within different fractures were 0.05 m/s.

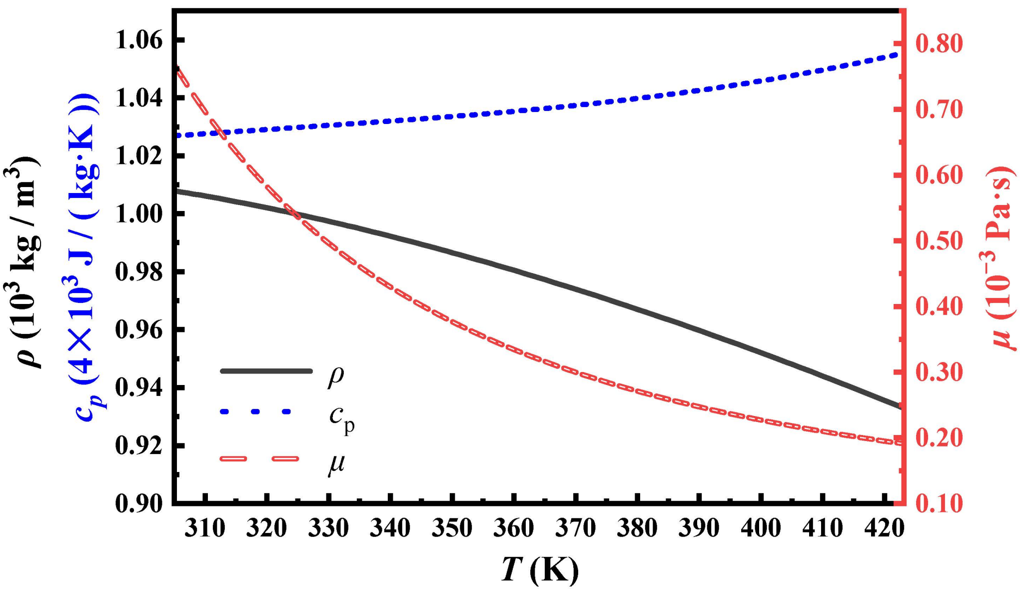

Figure 4. Thermal properties of water vary with temperature.

2.3. The Overall Heat Transfer Coefficient

The heat transfer coefficient has been established as a key parameter to evaluate the heat transfer ability between the flowing fluid and the rock [27], and it is affected by several factors including fracture type, flow rate, surface roughness, fracture aperture and infilling materials. The overall heat transfer coefficient (OHTC) represents a comprehensive parameter involved in the heat transfer process, taking into account the effects of solid surface heat transfer and fluid convection heat. This coefficient describes the efficiency of heat transfer throughout the entire single fracture [28]. It is commonly employed to assess and design heat exchange equipment, pipelines and other thermal transfer processes. Therefore, to comprehensively consider the influence of various factors on heat transfer within a single fracture, this study employed the OHTC for the associated computational analysis.

Researchers have developed several equations to calculate the heat transfer coefficient [5,10,29,42]. Considering the fact that the heat (Q) absorbed by water in the whole fracture pathway equals the heat transfer convection between the water and the inner surface of the fracture:

$$Q = Ah(T_c - T_w) = C_{Pf}\rho_f q_v(T_{out} - T_{in}) \tag{7}$$

where h is the overall heat transfer coefficient (OHTC) (W/m^2·K); A is the heat transfer surface area of rock fractures (m^2); T_c is the temperature at the outer wall surface of the fracture model (K); T_w is the temperature of the fluid in the fracture (K); q_v is the volumetric flow rate (ml/min); and T_{out} and T_{in} are the outlet and inlet temperatures of the water (K).

Assuming that the temperature along the radius of the model follows a linear function, the equivalent OHTC for a single rock fracture was calculated in this study according to Bai et al. [10],

$$h = \frac{C_{Pf}\rho_f q_v(T_{out} - T_{in})}{A(T_c - (T_{out} + T_{in})/2)} \tag{8}$$

The values of the above parameters can be obtained using the integral function in COMSOL™.

3. Numerical Verification

The tetrahedral elements are the main grid cells in the 3D model meshing, which provide flexibility to accommodate complex irregular geometries. The high-precision parameterized surface function in the COMSOL™ was also used to construct the irregular spatial structure sandwiched between the two rough fracture surfaces. Fine meshing was applied around both the inlet and outlet, as well as in the intricate boundary layer regions. After the grid elements were increased to 240,000, the outlet temperature of the fluid would no longer vary with the quantity, and about 300,000 grid elements were finally constructed in the numerical models to guarantee the accuracy of the calculation results.

The simulation results in this study have been compared with the detailed experimental data published to ensure the accuracy and reliability of the numerical model; more experimental results can be found in Ma et al.'s study [4]. The specimens in the experiment were produced as a cylinder, with a length of 100 mm and a diameter of 50 mm, through concrete casting. At the same time, ten samples with fractures of different inner surface roughness (JRCs of 2–20) were manufactured using 3D printing. The verification model of a single fracture in this study was established with the inner surface s0 (as shown in Figure 3) and a fracture aperture of 0.2 mm, which was taken from one of the experimental samples with JRCs of 16–18. All tests were conducted under consistent experimental conditions, including temperature control, permeation and confining pressure, closely replicating real geothermal reservoir environments. The experimental system collected and recorded the data on flow velocity, pressure and temperatures during the fluid flow and heat transfer process in the single fracture. The temperature of the fluid at the inlet and outlet was measured using resistance temperature detectors (RTDs) (Pt 100). With simulation parameters set exactly the same as the experimental conditions, eight simulation models were performed according to the experiment process at volumetric flow rates of 15 and 20 mL/min, and the outer wall surface temperature increased from 333.15 to 363.15 K. The final record was taken when the temperature reached a steady state. Furthermore, to better replicate the testing conditions, the average temperature in the range of 20 × 0.1 mm at the center of the fracture outlet was taken as the simulation result of T_{out}.

A comparison between the outlet temperature obtained by the simulation and the experimental results is presented in Figure 5. As shown, the simulation results of the outlet temperature are in good agreement with the experimental data. In all eight cases, the relative errors of T_{out} are all no more than 6% [23], with a maximum relative error of 4.66%. This is also consistent with the validation findings from the related study conducted by Ma et al. [7]. Therefore, the model can be considered accurate for the simulation in this study, and the simulation results are fully reliable.

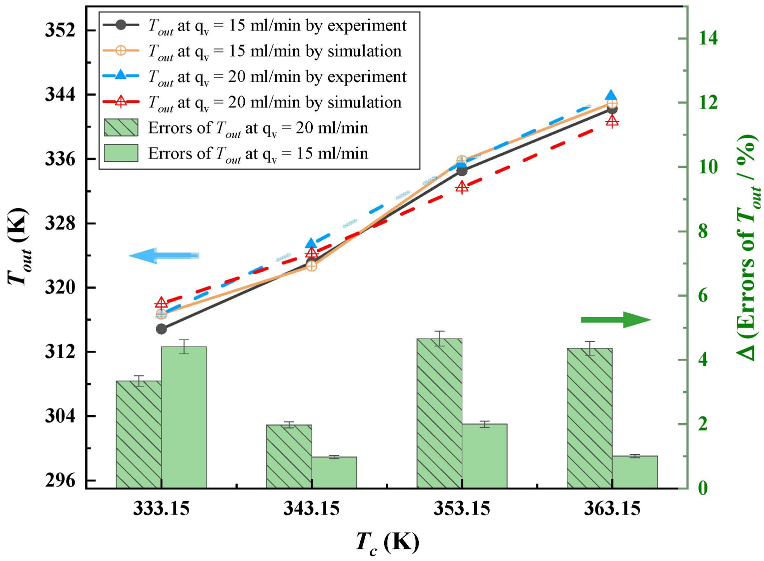

Figure 5. The errors of T_{out} between experiment and simulation results under different volume flow rates ($\Delta = \frac{|T_{out,si} - T_{out,ex}|}{T_{out,ex} - 273.15}$, $T_{out,si}$ and $T_{out,ex}$ are the results of T_{out} by simulation and experiment) (The colored arrows point to the corresponding Y-axes for T_{out} and errors.).

4. Results and Discussion

4.1. Effect of Fracture Inner Surface Morphology on Flow Heat Transfer

Figure 6 illustrates the variations in internal flow heat transfer for four different fracture surface morphologies with an aperture of 0.2 mm. The heat transfer medium remains water, with an inlet temperature of 313.15 K, and rock temperature and pressure are constant at 373.15 K and 30 MPa. The calculation of the OHTC for the single fracture was based on Equation (8).

As the flow velocity of the heat transfer medium was increased from 0.01 m/s to 0.18 m/s, the OHTC within a single fracture exhibited an exponential growth. This is in complete accordance with the proportional relationship between flow velocity 'v' and convective heat transfer intensity in forced convection heat transfer. With the higher flow velocity of the heat transfer medium, the convective term in the heat transfer process becomes more significant, resulting in improved overall convective heat transfer efficiency, provided that the thermal conductivity remains constant. However, the outlet temperature of the heat transfer medium after convective heat transfer would exhibit a weak exponential decrease with increasing flow velocity. For single fracture models with the same dimensions and other conditions, they could achieve the same total heat exchange at steady state. A higher flow velocity could result in a smaller temperature difference at the inlet and outlet of the heat transfer medium.

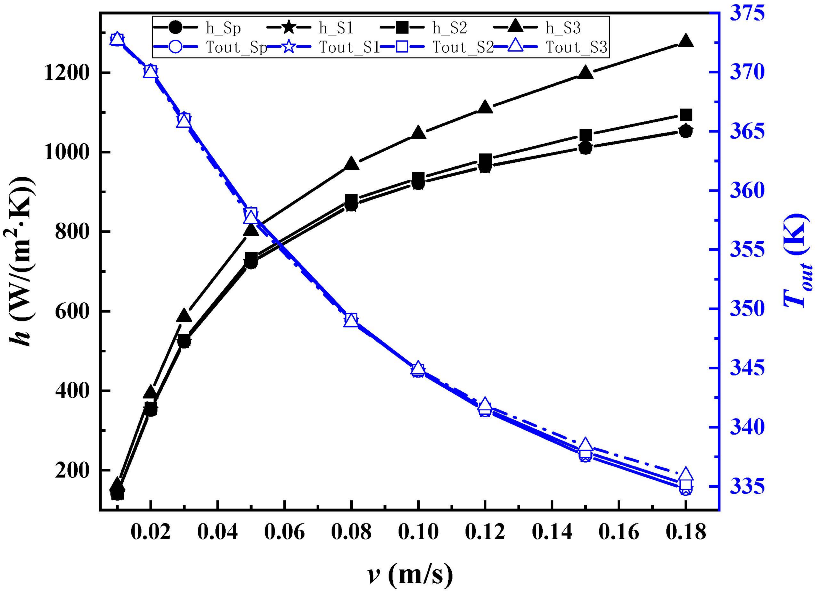

Figure 6. Variation in the OHTC and Tout with flow rate for four fracture surface models (b = 0.2 mm).

When the internal surface morphology of the single fracture varied, the extent of the increase in h and decrease in T_{out} could differ. Amongst the four fracture surfaces of sp, s1, s2 and s3, the fractures with rougher inner surfaces were observed to exhibit a greater increase in the OHTC. Particularly, the OHTC in a single fracture with an inner surface s3 can be up to 1.215 times that of a parallel flat fracture when the flow velocity reaches 0.18 m/s. Moreover, at a high flow velocity, the influence of roughness on the OHTC became more pronounced. Rougher fluids produced greater resistance within the fracture. These fluids possess higher molecular kinetic energy, longer residence times and better heat transfer efficiency. The results align with the known impact of roughness on forced convection heat transfer within confined spaces [7], indicating that in this study, the effect of surface roughness on heat transfer with fracture inner walls under smaller apertures should not be overlooked. However, different fracture morphologies have a relatively small overall impact on T_{out}. Therefore, roughness has a minor influence on the overall heat exchange within a single fracture, which is directly related to the steady-state calculations and geometric dimensions of the model in this study.

The distribution contours of rock temperature under different fracture surface morphology with flow velocities of 0.03, 0.05 and 0.08 m/s are plotted in Figure 7. These contours were obtained from the YZ cross-section at the center of the four single fracture models with an aperture of 0.2 mm. As seen in the figure, the temperature distribution inside the rock is directly affected by the water flow and the morphology of the single fracture inner surface. From Figure 7a–c, as the roughness of the fracture inner surface increases from a parallel plate to a D value of 2.09, disturbances occur at the upper and lower boundaries of the fracture for fluid intensify, leading to fluctuations in the temperature distribution contours near the fracture surfaces. This effect becomes more obvious as the flow velocity increases, which means that the effect of roughness is gradually accentuated. This indicates that the morphological characteristics of different fracture inner surfaces can significantly affect the direction and magnitude of the coupled fluid–solid heat transfer within the rock, and it is especially more pronounced at higher flow velocities. However, a higher velocity leads to a reduction in heat transfer time within the fractures, ultimately resulting in a decrease in heat absorption and outlet temperature. Consequently, the selection and optimization of the working fluid flow parameters are crucial for the efficient extraction of heat from deep geothermal reservoirs.

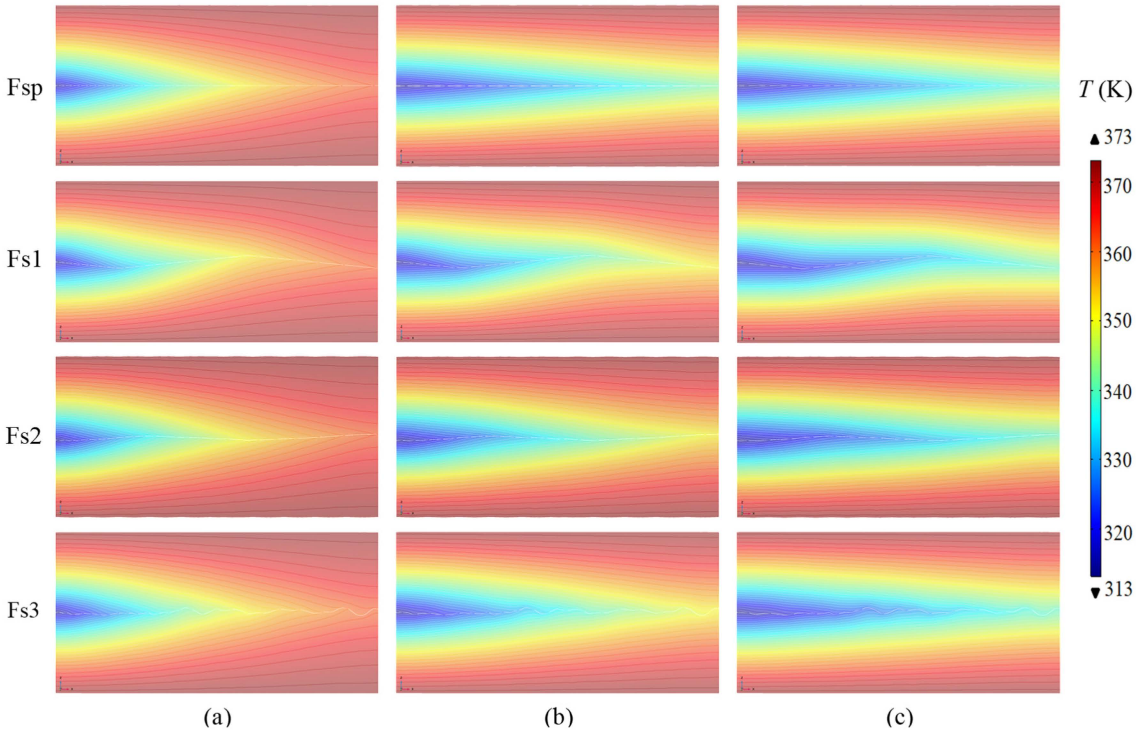

Figure 7. Rock temperature distribution contours under different fracture surface morphologies at the flow velocity (**a**) v = 0.03 m/s, (**b**) v = 0.05 m/s, (**c**) v = 0.08 m/s (b = 0.2 mm).

In additionally, the state of rock temperature distribution in the simulation results of this study is consistent with that of He et al. [25] and Heinza et al. [43], which further validates the effectiveness of our numerical model.

4.2. Effect of Roughness Fracture Characteristics on Flow Heat Transfer

The geometric parameters for a single fracture channel are also the main factors affecting the heat transfer rate and efficiency. In order to better understand the factors influencing the OHTC of a single fracture, the CFA proposed in Section 2.1 was employed to comprehensively characterize the geometric aperture and inner surface roughness of the single fracture.

Figure 8 displays the rock temperature distribution contours for the single fracture Fs3 with a rough inner surface, under different configurations of three CFAs (apertures of 0.3, 0.4 and 0.5 mm) and three water flow velocities (0.03, 0.05 and 0.08 m/s). The results of the temperature distribution for the same fracture under a CFA of 0.21 (aperture of 0.2 mm) and the same flow velocity conditions have been shown in Figure 7. As seen in both Figures 7 and 8, the variation region of rock temperature distribution that is affected by the low-temperature fluid flowing for the heat extraction expands as the flow velocity and the fracture aperture increase. This indicates that both an increase in fracture aperture and flow velocity offers a significant enhancement in improving the performance of convective heat transfer. However, an excessively large aperture can result in a non-negligible for the normal heat conduction and temperature differences of the fluid within the fracture, which can affect the unit heat input of the fluid and ultimately the outlet temperature. The volume flow rate of the fluid in Figure 8 is equal for b = 0.50 mm in plot Figure 8a and b = 0.30 mm in plot Figure 8b. Comparison of the results between the two plots reveals that the former has a greater range of fluid effects on the temperature distribution of the rock, while the latter has more pronounced inlet effects. This indicates that enhancing the fracture aperture has a more sensitive effect on improving heat transfer performance. Therefore, the creation of fractures with larger apertures should be the primary goal in the initial stages of reservoir development.

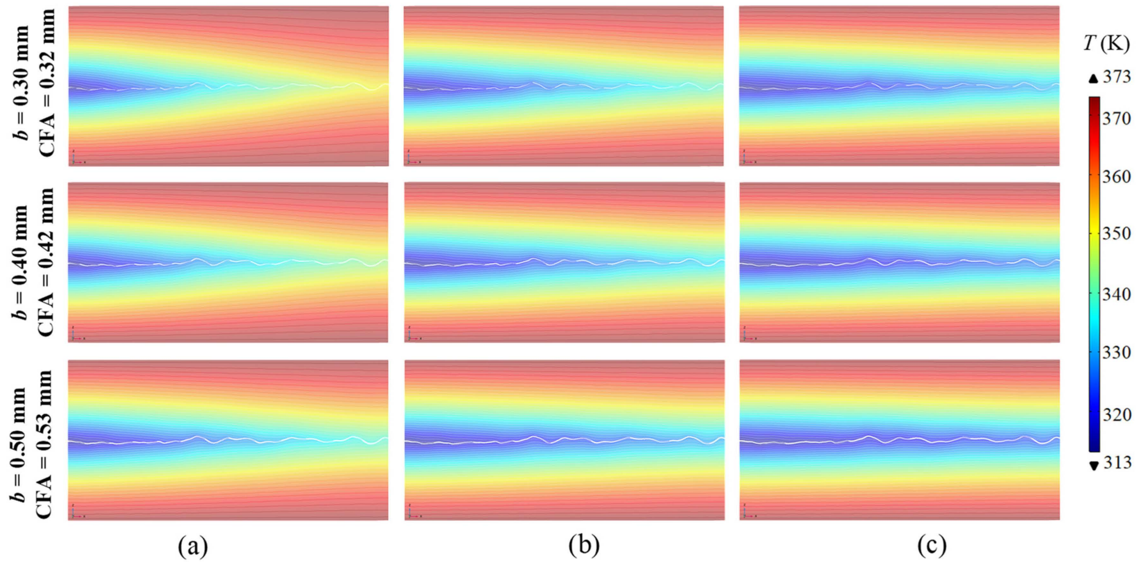

Figure 8. Rock temperature distribution contours of Fs3 with different apertures and flow velocities: (**a**) v = 0.03 m/s, (**b**) v = 0.05 m/s, (**c**) v = 0.08 m/s.

The OHTC formula was further used to explore the influence of fracture channel geometry parameters on fluid–solid-coupled heat transfer by comparing the calculation results of the single fracture models Fsp and Fs3. Figure 9 illustrates the effects of CFAs on outlet temperature and OHTC amongst the single fractures Fsp and Fs3, under three velocities of 0.03 m/s, 0.05 m/s and 0.08 m/s. The CFA values in the horizontal axis of the figure were all from the calculation results corresponding to the aperture at 0.1 to 0.5 mm for the two single fractures. According to the definition of CFA in Equation (1), the values of CFA indirectly reflected the degree of the aperture and the roughness of the inner wall surface for the single fracture, which was a mixed parameter. Obviously, the values of CFA for Fsp were equal to the aperture values, while that of Fs3 was slightly larger than the corresponding aperture value. The results from the plots of Figure 9(a1,b1,c1) show that the OHTCs of both single fractures were increased with the CFA, and the amplitude of the OHTC increase tended to flatten with the CFA, which indicated the existence of a critical CFA that made the OHTC close to the maximum value at different velocities. While the OHTC is more sensitive to the change in CFA at small values, this means the critical CFA is larger for smaller velocities or rougher single fractures. This is directly related to the fact that a larger aperture would cause a larger CFA, which leads to a higher flow rate. The roughness, on the other hand, has a boosting effect on the threshold value of the CFA that would slow down the OHTC change; therefore, the rougher the single fracture, the wider the interval of CFA sensitivity. The OHTC of Fs3 was generally larger than that of Fsp, especially at higher velocities where the difference was greater. This demonstrated the positive effect of roughness on the improvement in OHTC within a single fracture and showed that it is more pronounced at increased flow velocities.

As shown in Figure 9(a2,b2,c2), the fluid temperature T_{out} at the exit of both the Fsp and Fs3 fractures declined significantly with an increasing CFA, and the higher the fluid flow velocity, the smaller the decrease in T_{out}, which was more sensitive to small CFA changes. This was mainly due to the fact that the main role in the CFA change was affected by the degree of aperture when the fluid in the single fracture was at low flow velocity; the increase in the aperture made the flow fluid per unit volume of heat transfer smaller, that is, the T_{out} was closer to the T_{in}. At this time, compared to the degree of aperture, the ability of surface roughness to improve the heat transfer in the single fracture is very limited; a change in the aperture shows a more significant impact on the fluid–solid-coupling heat transfer effect within a single fracture. However, after an increase in the flow velocity, the OHTC and T_{out} of Fs3 under high-velocity conditions were significantly higher than that of Fsp. Within the same CFA change interval, the decrease in the T_{out} at 0.08 m/s was less than that at 0.03 m/s by 18.33%. This was mainly because, under high-velocity conditions, the fluid near the rough inner wall surface of the single fracture was more prone to a change in the flow state and an increase in the heat transfer. At this time, the influence of the aperture in the CFA on heat transfer gradually declined, and the influence of roughness gradually became prominent. Therefore, using CFA values is convenient for quantifying the main geometric characteristics of a single fracture, and they can comprehensively characterize the coupled influence of the aperture and inner wall roughness on heat transfer in a single fracture.

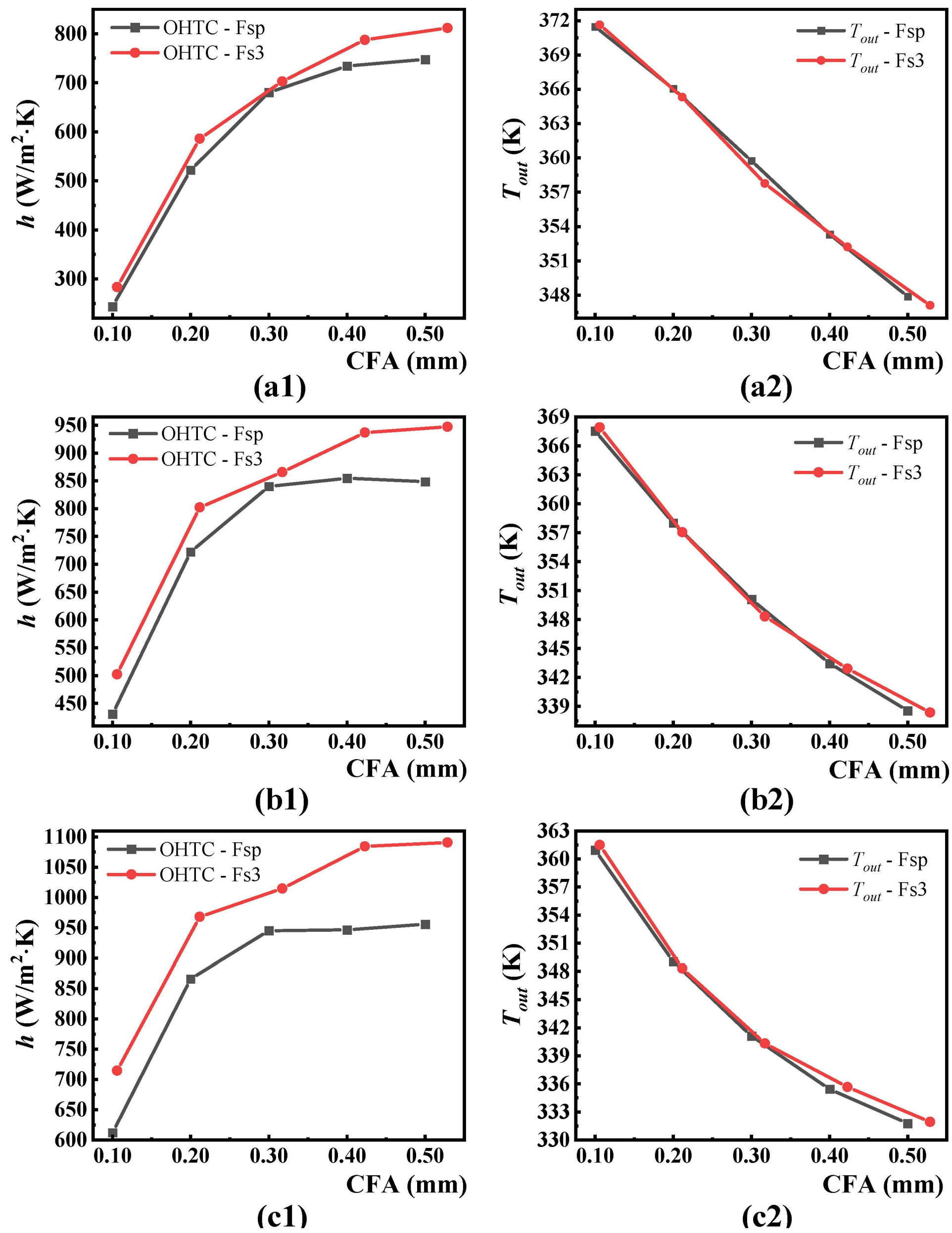

Figure 9. Effects of CFA on outlet temperature and OHTC amongst the fractures Fsp and Fs3, under three velocities of 0.03 m/s (**a1**,**a2**), 0.05 m/s (**b1**,**b2**) and 0.08 m/s (**c1**,**c2**).

4.3. Heat Transfer Correlations in a Single Fracture

In the studies of convective heat transfer, similarity criteria serve as the foundation for conducting a series of experiments. Hence, establishing a functional relationship between dimensionless criteria, organized by the results and data from related studies, has better versatility and value for engineering applications. According to the theory of dimensional analysis, the *Nu* is related to *Re* and *Pr*, and these criteria numbers can be obtained through calculations based on the conditions and results of the simulation cases. For the four models (Fs1, Fs2, Fs3 and Fsp) with a constant aperture of 0.2 mm, scatter plots of the relationship between *Re* and $Nu/Pr^{1/3}$ as the flow velocity varies from 0.01 to 0.18 m/s are presented in Figure 10, where $Nu/Pr^{1/3}$ serves as a conventional preprocessing term in the experimental correlation equations.

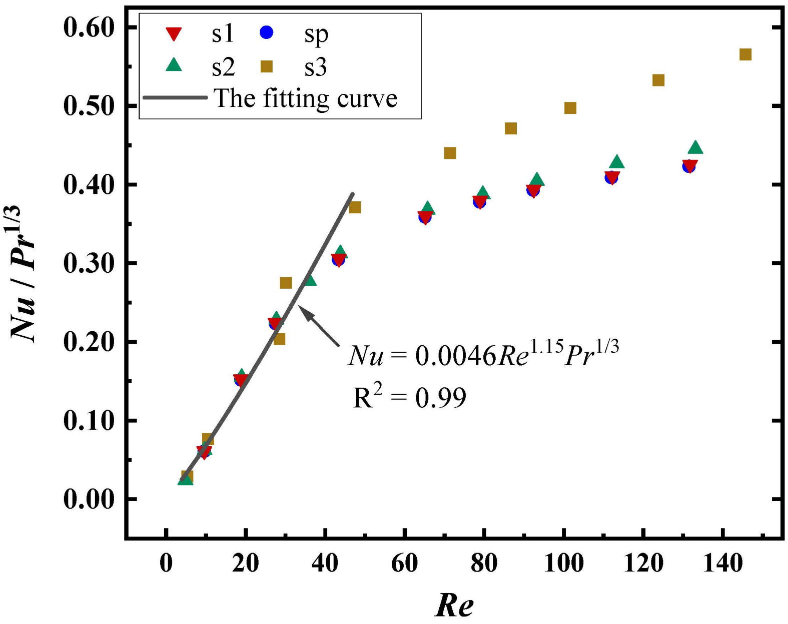

Figure 10. The relationship between *Re* and $Nu/Pr^{1/3}$.

As is visible, *Nu* was jointly influenced by *Re* and *Pr*, which showed a positive relationship. When the *Re* was small, the fluid flow within the fracture was laminar; the correlation between the average *Nu* and the *Re*, *Pr* of the fracture showed a low sensitivity to the different models. It indicated that roughness has little effect on the enhancement of the heat transfer capacity within a single fracture. Thus, when $Re < 60$, there is a certain curvilinear relationship between *Re* and $Nu/Pr^{1/3}$ that is consistent with the heat transfer law. After fitting, the curvilinear relationship that is conformed for all four models is:

$$Nu = 0.0046Re^{1.15}Pr^{\frac{1}{3}} \tag{9}$$

With a rise in *Re* value, the curvilinear relationship was no longer strictly followed. When the $Re > 60$, the relationship between *Re*, *Nu* and *Pr* in the different single fracture models was no longer consistent and showed a trend related to the model characteristics. As shown, Fsp has the smallest *Nu*, followed by Fs1 and Fs2. Fs3 has the largest *Nu*, which is consistent with the relationship between the roughness characteristics of the fracture surfaces of the four models. This also indicates that the relative value of convective heat transfer capacity over thermal conductivity in the fracture was increased with the increasing roughness of the inner wall surface. This provides further evidence of the positive effect of inner wall surface roughness on enhancing convective heat transfer capacity within a single fracture, which was more prominent at a higher *Re*.

Although Equation (9) was developed based on a series of numerical simulation results, its reliability requires further validation through relevant experiments on fluid flow and heat transfer within a single fracture. Furthermore, the model for coupled fluid–solid heat transfer needs additional refinement for future applications in engineering simulations.

5. Conclusions

In order to further understand the characteristics of fluid flow and heat transfer in a single fracture, simulations have been implemented for the heat transfer process within a single fracture under different geometric features and flow conditions in this study. With the analysis of the results, the main findings are as follows:

1. As the fluid velocity within a single fracture increases, the OHTC increases significantly. Moreover, the greater roughness of the fracture inner surface enhances the heat transfer capability; the OHTC in a single fracture with an inner surface fractal dimension of 2.09 can be up to 1.215 times that of a parallel flat fracture when the flow velocity reaches 0.18 m/s. However, excessively high velocities lead to a reduction in heat transfer time within the fractures, ultimately resulting in a decrease in heat absorption and outlet temperature. Consequently, optimizing the flow parameters of the working fluid is paramount for efficient heat extraction.
2. The overall heat transfer coefficient (OHTC) increases with an increase in compound fracture aperture (CFA), indicating that both a rise in fracture aperture and roughness could effectively increase the OHTC. For a smaller CFA, enhancing the fracture aperture could have a decisive role in increasing the OHTC, but as the aperture reached a certain level, the influence of fracture surface roughness would gradually become more evident. Therefore, in the initial stage of reservoir development, creating fractures with larger apertures should be the primary goal, and the aperture emerges as a more sensitive optimization parameter for efficient heat extraction compared to the flow velocity.
3. A correlation equation for flow and heat transfer characteristics within fractures (when $Re < 60$) has been derived, which provides more accurate estimates of the OHTC in rock fractures with different geometries and morphological features.

Author Contributions: D.L.: Conceptualization, Methodology, Validation, Writing—original draft preparation. G.L.: Writing—review and editing, Resources, Supervision, Funding acquisition. S.L.: Supervision, Resources. All authors have read and agreed to the published version of the manuscript.

Funding: This work was funded by the National Natural Science Foundation of China [52076218].

Data Availability Statement: The data presented in this study are available on request from the corresponding author.

Conflicts of Interest: The authors declare no conflicts of interest.

References

1. Olasolo, P.; Juárez, M.C.; Morales, M.P.; D'Amico, S.; Liarte, I.A. Enhanced geothermal systems (EGS): A review. *Renew. Sustain. Energy Rev.* **2016**, *56*, 133–144. [CrossRef]
2. Liu, G.; Yuan, Z.; Zhou, C.; Fu, Z.; Rao, Z.; Liao, S. Heat extraction of enhanced geothermal system: Impacts of fracture topological complexities. *Appl. Therm. Eng.* **2023**, *219*, 119236. [CrossRef]
3. Liu, G.; Zhou, C.; Rao, Z.; Liao, S. Impacts of fracture network geometries on numerical simulation and performance prediction of enhanced geothermal systems. *Renew. Energy* **2021**, *171*, 492–504. [CrossRef]
4. Ma, Y.; Zhang, Y.; Hu, Z.; Yu, Z.; Huang, Y.; Zhang, C. Experimental study of the heat transfer by water in rough fractures and the effect of fracture surface roughness on the heat transfer characteristics. *Geothermics* **2019**, *81*, 235–242. [CrossRef]
5. Chen, Y.; Zhao, Z. Heat transfer in a 3D rough rock fracture with heterogeneous apertures. *Int. J. Rock Mech. Min. Sci.* **2020**, *134*, 104445. [CrossRef]
6. Zhao, J.; Tso, C.P. Heat transfer by water flow in rock fractures and the application to hot dry rock geothermal systems. *Int. J. Rock Mech. Min. Sci. Geomech. Abstr.* **1993**, *30*, 633–641. [CrossRef]
7. Ma, Y.; Zhang, Y.; Yu, Z.; Huang, Y.; Zhang, C. Heat transfer by water flowing through rough fractures and distribution of local heat transfer coefficient along the flow direction. *Int. J. Heat Mass Transf.* **2018**, *119*, 139–147. [CrossRef]
8. Li, Z.-W.; Feng, X.-T.; Zhang, Y.-J.; Zhang, C.; Xu, T.-F.; Wang, Y.-S. Experimental research on the convection heat transfer characteristics of distilled water in manmade smooth and rough rock fractures. *Energy* **2017**, *133*, 206–218. [CrossRef]
9. Luo, Y.; Xu, W.; Lei, Y.; Wu, P.; Qin, G.; Ba, R. Experimental study of heat transfer by water flowing through smooth and rough rock fractures. *Energy Rep.* **2019**, *5*, 1025–1029. [CrossRef]

10. Bai, B.; He, Y.; Li, X.; Li, J.; Huang, X.; Zhu, J. Experimental and analytical study of the overall heat transfer coefficient of water flowing through a single fracture in a granite core. *Appl. Therm. Eng.* **2017**, *116*, 79–90. [CrossRef]
11. Bai, B.; He, Y.; Hu, S.; Li, X. An Analytical Method for Determining the Convection Heat Transfer Coefficient Between Flowing Fluid and Rock Fracture Walls. *Rock Mech. Rock Eng.* **2017**, *50*, 1787–1799. [CrossRef]
12. Huang, Y.; Zhang, Y.; Yu, Z.; Ma, Y.; Zhang, C. Experimental investigation of seepage and heat transfer in rough fractures for enhanced geothermal systems. *Renew. Energy* **2019**, *135*, 846–855. [CrossRef]
13. He, Y.; Bai, B.; Hu, S.; Li, X. Effects of surface roughness on the heat transfer characteristics of water flow through a single granite fracture. *Comput. Geotech.* **2016**, *80*, 312–321. [CrossRef]
14. Luo, J.; Qi, Y.; Zhao, Q.; Tan, L.; Xiang, W.; Rohn, J. Investigation of Flow and Heat Transfer Characteristics in Fractured Granite. *Energies* **2018**, *11*, 1228. [CrossRef]
15. Li, J.; Ma, W.; Jiang, P.; Xu, R. Heat transfer characterizations of water flow through a single fracture with integrating water dissolution effects for the Enhanced Geothermal Systems. *Appl. Therm. Eng.* **2024**, *239*, 122133. [CrossRef]
16. Shu, B.; Zhu, R.; Elsworth, D.; Dick, J.; Liu, S.; Tan, J.; Zhang, S. Effect of temperature and confining pressure on the evolution of hydraulic and heat transfer properties of geothermal fracture in granite. *Appl. Energy* **2020**, *272*, 115290. [CrossRef]
17. Frank, S.; Heinze, T.; Pollak, S.; Wohnlich, S. Transient heat transfer processes in a single rock fracture at high flow rates. *Geothermics* **2021**, *89*, 101989. [CrossRef]
18. Barton, N. Review of a New Shear-strength Criterion for Rock Joints. *Eng. Geol.* **1973**, *7*, 287–332. [CrossRef]
19. Gao, X.-F.; Zhang, Y.-J.; Huang, Y.-B.; Zhao, Y.; Ni, J.; Ma, J.-C. Numerical simulation of convective heat transfer characteristics of a rough single fracture in granite. *Rock Soil Mech.* **2020**, *41*, 1761–1769.
20. Zhang, Y.-Z.; Sun, C.; Bao, Y.; Zhou, Q. How surface roughness reduces heat transport for small roughness heights in turbulent Rayleigh–Bénard convection. *J. Fluid Mech.* **2017**, *836*, R2. [CrossRef]
21. Zhang, Q.; Luo, S.; Ma, H.; Wang, X.; Qian, J. Simulation on the water flow affected by the shape and density of roughness elements in a single rough fracture. *J. Hydrol.* **2019**, *573*, 456–468. [CrossRef]
22. Ji, Y.; Yuan, K.; Chung, J.N. Numerical simulation of wall roughness on gaseous flow and heat transfer in a microchannel. *Int. J. Heat Mass Transf.* **2006**, *49*, 1329–1339. [CrossRef]
23. Shishkina, O.; Wagner, C. Modelling the influence of wall roughness on heat transfer in thermal convection. *J. Fluid Mech.* **2011**, *686*, 568–582. [CrossRef]
24. Thompson, M.E.; Brown, S.R. The effect of anisotropic surface roughness on flow and transport in fractures. *J. Geophys. Res. Solid Earth* **1991**, *96*, 21923–21932. [CrossRef]
25. He, R.; Rong, G.; Tan, J.; Cheng, L. Numerical investigation of fracture morphology effect on heat transfer characteristics of water flow through a single fracture. *Geothermics* **2019**, *82*, 51–62. [CrossRef]
26. He, R.; Rong, G.; Tan, J.; Phoon, K.-K. Analytical and numerical study on heat transfer coefficient between rock fracture walls and flowing fluid. *Geothermics* **2021**, *95*, 102122. [CrossRef]
27. Bedre, M.G.; Anderson, B.J. Sensitivity analysis of low-temperature geothermal reservoirs: Effect of reservoir parameters on the direct use of geothermal energy. *GRC Trans.* **2012**, *36*, 7.
28. Bai, B.; He, Y.Y.; Li, X.C. Numerical study on the heat transfer characteristics between supercritical carbon dioxide and granite fracture wall. *Geothermics* **2018**, *75*, 40–47. [CrossRef]
29. Zhao, Z. On the heat transfer coefficient between rock fracture walls and flowing fluid. *Comput. Geotech.* **2014**, *59*, 105–111. [CrossRef]
30. Zhang, L.; Jiang, P.; Wang, Z.; Xu, R. Convective heat transfer of supercritical CO_2 in a rock fracture for enhanced geothermal systems. *Appl. Therm. Eng.* **2017**, *115*, 923–936. [CrossRef]
31. Bai, B.; He, Y.; Li, X.; Hu, S.; Huang, X.; Li, J.; Zhu, J. Local heat transfer characteristics of water flowing through a single fracture within a cylindrical granite specimen. *Environ. Earth Sci.* **2016**, *75*, 1460. [CrossRef]
32. Xie, H.P.; Sun, H.Q.; Ju, Y.; Feng, Z.G. Study on generation of rock fracture surfaces by using fractal interpolation. *Int. J. Solids Struct.* **2001**, *38*, 5765–5787. [CrossRef]
33. Li, B.; Liu, R.; Jiang, Y. Influences of hydraulic gradient, surface roughness, intersecting angle, and scale effect on nonlinear flow behavior at single fracture intersections. *J. Hydrol.* **2016**, *538*, 440–453. [CrossRef]
34. Tzelepis, V.; Moutsopoulos, K.N.; Papaspyros, J.N.E.; Tsihrintzis, V.A. Experimental investigation of flow behavior in smooth and rough artificial fractures. *J. Hydrol.* **2015**, *521*, 108–118. [CrossRef]
35. Ranjith, P.G. An experimental study of single and two-phase fluid flow through fractured granite specimens. *Environ. Earth Sci.* **2010**, *59*, 1389–1395. [CrossRef]
36. Shen, S.; Xu, J.L.; Zhou, J.J.; Chen, Y. Flow and heat transfer in microchannels with rough wall surface. *Energy Conv. Manag.* **2006**, *47*, 1311–1325. [CrossRef]
37. Jarrahi, M.; Holländer, H. Numerical simulation of flow heterogeneities within a real rough fracture and its transmissivity. *Energy Procedia* **2017**, *125*, 353–362. [CrossRef]
38. Yu, L.Y.; Liu, R.C.; Jiang, Y.J. A Review of Critical Conditions for the Onset of Nonlinear Fluid Flow in Rock Fractures. *Geofluids* **2017**, *2017*, 2176932. [CrossRef]
39. Xing, K.; Qian, J.; Zhao, W.; Ma, H.; Ma, L. Experimental and numerical study for the inertial dependence of non-Darcy coefficient in rough single fractures. *J. Hydrol.* **2021**, *603*, 127148. [CrossRef]

40. Zhou, J.Q.; Hu, S.H.; Fang, S.; Chen, Y.F.; Zhou, C.B. Nonlinear flow behavior at low Reynolds numbers through rough-walled fractures subjected to normal compressive loading. *Int. J. Rock Mech. Min. Sci.* **2015**, *80*, 202–218. [CrossRef]
41. Rong, G.; Tan, J.; Zhan, H.; He, R.; Zhang, Z. Quantitative evaluation of fracture geometry influence on nonlinear flow in a single rock fracture. *J. Hydrol.* **2020**, *589*, 125162. [CrossRef]
42. Zhang, G.; Zhu, J.; Li, J.; Wang, Q. The analytical solution of the water–rock heat transfer coefficient and sensitivity analyses of parameters. In Proceedings of the World Geothermal Congress 2015, Melbourne, Australia, 19–24 April 2015.
43. Heinze, T.; Hamidi, S.; Galvan, B. A dynamic heat transfer coefficient between fractured rock and flowing fluid. *Geothermics* **2017**, *65*, 10–16. [CrossRef]